Conformational Analysis of Cyclohexane-derived Analogues of Glutamic Acid by X-Ray Crystallography, NMR Spectroscopy in Solution, and Molecular Dynamics

Nathalie Morelle,[a] Josyane Gharbi-Benarous,[a] Francine Acher,[a] Giovanni Valle,[b] Marco Crisma,[b] Claudio Toniolo,[b] Robert Azerad[a] and Jean-Pierre Girault*,[a]

[a] *Laboratoire de Chimie et Biochimie Pharmacologiques et Toxicologiques (URA 400 CNRS), Université René Descartes, 45 rue des Saints-Pères, 75270 Paris Cedex 06, France*

[b] *Biopolymer Research Center, C.N.R., Department of Organic Chemistry, University of Padova, 35131 Padova, Italy*

The conformational analysis of two glutamic acid analogues containing a cyclohexane ring, substituted in position 1 by an amino and a carboxy group, and in position 3 by a second carboxy group, has been investigated by X-ray crystallography, ^1H and ^{13}C NMR spectroscopy in an aqueous environment, and molecular dynamics (MD). These analogues exclusively exhibit chair conformations in aqueous solution. When the two carboxy groups are *cis* they are shown to be equatorial and the amino group axial, whatever the pH and the charge are. However, in the *trans*-isomer the 1-amino and 3-carboxy group are equatorial except around neutral pH, where there is an equilibrium with another conformer, in which the 1-ammonium and the 3-carboxylate groups are axial and stabilized by a large electrostatic interaction or hydrogen bond.

The introduction of conformationally restricted analogues of natural amino acids in substrates or inhibitors has proved helpful in studies of the geometry of binding sites;[1] *cis*- and *trans*-1-aminocyclohexane-1,3-dicarboxylic acids, hereafter named *cis*-C6 **1** and *trans*-C6 **2**, respectively (Fig. 1), have already been tested for some biological properties in comparison to glutamic acid: the *cis*-isomer **1** is a substrate of glutamine synthetase while the *trans*-form **2** is not active.[2] In the central nervous sytem the *cis*-isomer **1** has been shown to be an effective excitatory transmitter, and the *trans*-form **2** to be much less active.[3] Finally, enzymatic tests are under investigation on compounds derived from these amino acids in the vitamin K-dependent carboxylation reaction.[4]

To be able to determine structure–activity relationships, we have undertaken a study of the conformation of *cis*-**1** and *trans*-**2** -C6,[5] for which the stable conformations expected are limited to one or two chair conformations. For instance, the *cis*-isomer at isoelectric pH may adopt one of the two conformations represented in Fig. 2, with, in the **a** conformer, the amino group axial and in the **b** conformation the amino group equatorial.

However, as three acidity functions are present in these compounds, the charges of the groups and their protonation depend on the pH of the solution: four predominant forms must be taken into account for the study in aqueous solution (from species **0** to **3**, Fig. 3). The preferred conformation may depend on these charges because of the electrostatic interactions or hydrogen bonding implied. We must then study each one of the 16 structures represented in Fig. 4: the first number indicates the isomer (*cis* **1**, *trans* **2**, see Fig. 1), the second one the predominant form in the pH zone considered (from acidic zone **0** to alkaline zone **3**, Fig. 3) and the letter the chair conformation (**a** or **b**, Fig. 2).

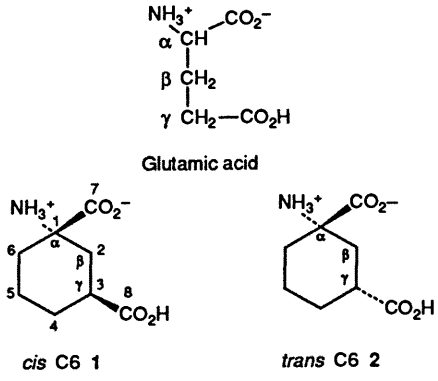

Fig. 1 Structure of the studied amino acids: glutamic acid, *cis*-C6 **1** and *trans*-C6 **2** (isomers α-*S* represented, zwitterions)

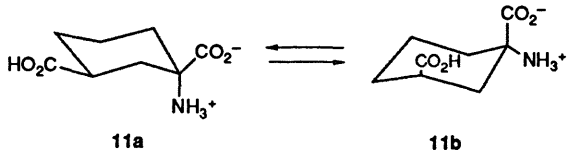

Fig. 2 **a** and **b** chair conformations for *cis*-C6 at isoelectric pH

Results and Discussion

X-Ray Crystallography.—The zwitterionic nature of the α-ammonium and α-carboxylate groups of *cis*-C6 **1** hemihydrate (Fig. 5) is strongly suggested by the lengths of the O(1)–C(7) and O(2)–C(7) bonds, 1.225(4) and 1.257(3) Å, respectively, for the α-carboxylate group. The corresponding values in the structure of the zwitterionic H_2^+–Acc^6–O^- (1-aminocyclohexane-1-carboxylic acid)[7] are 1.241(3) and 1.243(3) Å, whereas those in the structure of the protonated (Cl^-) H_2^+–Acc^6–OH molecule[8] are 1.317(14) and 1.219(14) Å. The γ-carboxylate group of compound **1** is protonated, the O(3)–C(8) and O(4)–C(8) bond distances being 1.215(4) and 1.300(4) Å, respectively.

The endocyclic cyclohexane ring torsion angles of compound **1** have a mean value of ± 53.8° (Table 1), to be compared with the mean value of ± 54.7° for a perfect chair conformation.[9] In addition, the total puckering amplitude Q (0.55 Å) is only slightly lower than that of an ideal cyclohexane chair (0.63 Å).[10] The magnitude of the distortion, given by tan θ [θ = 6.9(6)°],[10] is very small. As for the torsion angles relating the cyclohexyl ring of compound **1** to the substituents,[11] the (g^+, g^-) conformation (axial disposition) is adopted by the α-ammonium group, while the (t, t) conformation (equatorial disposition) is adopted by the α-carboxylate and γ-carboxy groups. Interestingly, in the H_2^+–Acc^6–O^- molecule[7] the α-carboxylate group occupies an axial position, whereas in the

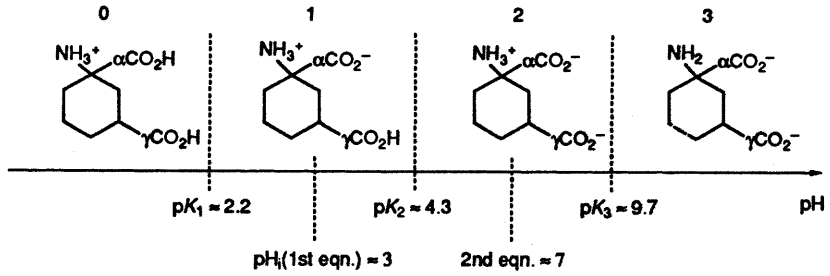

Fig. 3 Predominant forms of *cis*- and *trans*-C6 in the four pH zones (from **0** to **3**)

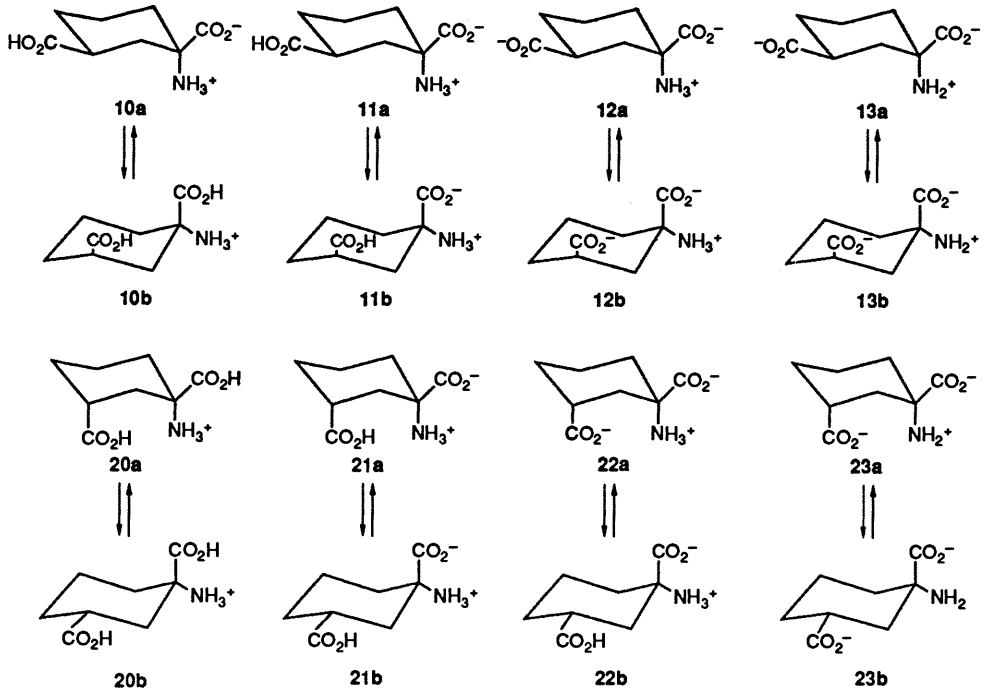

Fig. 4 Possible conformations for *cis*-**1** and *trans*-**2** C6 (α-*S* isomers represented)

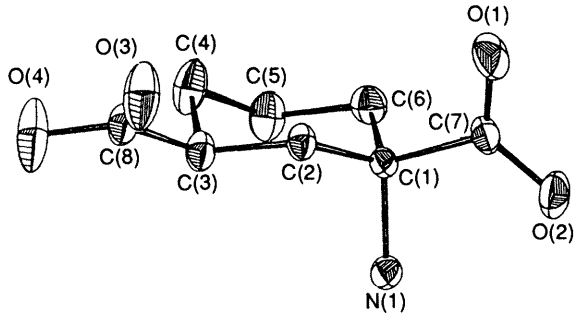

Fig. 5 An ORTEP (Johnson, 1976)[6] drawing of the *S,S* enantiomer of *cis*-C6 **1**. Non-hydrogen atoms are depicted as 50% probability ellipsoids.

Table 1 Torsion angles (°) for the *S,S*-enantiomer of *cis*-C6 **1** hemihydrate

O(1)–C(7)–C(1)–N(1)	−165.4(4)	C(2)–C(1)–C(6)–C(5)	−49.6(5)
O(2)–C(7)–C(1)–N(1)	17.3(6)	C(1)–C(6)–C(5)–C(4)	55.5(5)
O(2)–C(7)–C(1)–C(6)	−100.2(5)	C(6)–C(5)–C(4)–C(3)	−58.6(5)
O(1)–C(7)–C(1)–C(6)	77.1(5)	C(5)–C(4)–C(3)–C(2)	56.8(5)
O(2)–C(7)–C(1)–C(2)	136.8(5)	C(5)–C(4)–C(3)–C(8)	−179.2(4)
O(1)–C(7)–C(1)–C(2)	−45.9(6)	C(4)–C(3)–C(2)–C(1)	−53.2(5)
C(7)–C(1)–C(2)–C(3)	170.7(4)	C(4)–C(3)–C(8)–O(4)	59.4(6)
N(1)–C(1)–C(2)–C(3)	−71.1(5)	C(4)–C(3)–C(8)–O(3)	−121.7(5)
C(7)–C(1)–C(6)–C(5)	−172.3(4)	C(2)–C(3)–C(8)–O(3)	1.8(7)
N(1)–C(1)–C(6)–C(5)	71.0(5)	C(2)–C(3)–C(8)–O(4)	−177.1(4)
C(6)–C(1)–C(2)–C(3)	49.1(5)	C(8)–C(3)–C(2)–C(1)	−176.5(4)

(Cl⁻) H_2^+–Acc[6]–OH molecule it is the α-ammonium group that occupies an axial position.[8]

In the crystal the molecules of compound **1** generate dimers *via* intermolecular H-bonds involving the γ-carboxy group. The O(4)···O(3)($-x, -1-y, -1-z$) distance is 2.645(4) Å. The water molecule forms H-bonds with the α-ammonium and α-carboxylate groups. The N(1)···O(w) ($1/2+x, y-1/2, z$) and O(w)···O(2) (x, y, z) distances are 2.972(4) and 2.885(3) Å, respectively. The two additional H-atoms of the α-ammonium group are linked to the two oxygen atoms of the α-carboxylate group forming rows of molecules along the **a**, **b** and the **b** directions, respectively. The N(1)···O(1) ($1/2+x, 1/2+y, z$) and N(1)···O(2) ($-x-1/2, 1/2+y, -z-1/2$) separations are 2.754(4) and 2.826(4) Å, respectively. The most probable range for an O···O H-bond in carboxylic acids is 2.7–2.8 Å,[12,13] while that for an (ammonium) N···O (carbonyl) H-bond is 2.8–2.9 Å.[14–16]

NMR Spectroscopy.—The study was made on samples dissolved in deuterium oxide at room temperature (see Experimental section). Several pHs are considered, except for the carbon resonances which are examined only at pH 7 due to solubility constraints and to the peculiar interest of this pH. The assignments have been made using 1D ^1H and ^{13}C (^1H decoupled and DEPT-135)[17] spectra, and 2D homonuclear (COSY-60)[18] and heteronuclear (F1 decoupled)[19] shift correlations. The results are presented in Tables 2 and 3. The well known characteristics of cyclohexane derivatives are recognizable in the spectra: equatorial protons have higher resonance frequencies and smaller ^3J $^1H,^1H$ coupling constants than do

Table 2 ^{1}H Chemical shifts in D_2O at various pH values (δ/[$^2H_4$]TSP error 0.01 ppm except * 0.05 ppm, ** 0.2 ppm, due to superpositions)

	cis-C6 **1**				*trans*-C6 **2**			
^{1}H	**10** pH 1.6	**11** pH 3.3	**12** pH 7.0	**13** pH 13.3	**20** pH 1.7	**21** pH 4.0	**22** pH 7.0	**23** pH 11.0
2 ax	2.08	1.96	2.01	1.72	1.75	1.59	1.67	1.30**
eq	2.08	1.96	2.02	1.72	2.46	2.15	1.99	2.18
3 ax	2.53	2.43	2.33	2.40	3.00	2.80	2.58	2.32
4 ax	1.39	1.35*	1.38	1.30	1.41	1.35	1.47	1.30**
eq	1.94	1.93*	1.97	1.87	2.05	1.80	1.67	1.84
5 ax	1.43	1.35*	1.47	1.53	1.72	1.55**	1.47	1.30**
eq	1.80	1.80	1.86	1.68*	1.85	1.55**	1.53	1.71
6 ax	1.90	1.75*	1.85*	1.53	1.65	1.55**	1.53	1.30**
eq	1.90	1.75*	1.90*	1.70*	2.24	1.96	1.90	2.04

Table 3 ^{13}C Chemical shifts in D_2O at pH 7 (δ_C/$SiMe_4$)

^{13}C	*cis*-C6 **12**	*trans*-C6 **22**
1	64.2	62.6
2	36.9	35.9
3	43.5	44.5
4	30.7	30.4
5	22.3	22.0
6	33.2	34.8
7	185.7	187.1
8	179.5	179.7

Table 4 ^{1}H,^{1}H coupling constants in D_2O (Hz, error 0.5 Hz); 3-H: noted axial or equatorial according to the predominant conformer (see the text). Values obtained by simulation of the signals for *cis*-C6 **12**

		cis-C6 **1**	*trans*-C6 **2**			
		12 pH 7.0	**20** pH 1.7	**21** pH 4.0	**25** pH 7	**23** pH 11
$^2J_{ax,eq}$	2ax,2eq	−13.0	−13.2		−14.5	
	4ax,4eq	−13.0	−12.6		−14.5	
	5ax,5eq	−13.3	−13.2			
	6ax,6eq	−13.0	−12.3			
$^3J_{ax,ax}$	2ax,3ax	11.8	11.8	9.7		11.4
	3ax,4ax	11.9	11.9	9.7		11.4
	4ax,5ax	12.0	12.3			
	5ax,6ax	12.0	12.4			
$^3J_{ax,eq}$	2ax,3eq				5.2	
	2eq,3ax	3.4	3.9	4.5		3.7
	3ax,4eq	3.4	4.0	4.5		3.7
	3eq,4ax				5.2	
	4ax,5eq	3.2	3.9			
	4eq,5ax	3.4				
	5ax,6eq	3.4				
	5eq,6ax	3.4	4.0			
$^3J_{eq,eq}$	2eq,3eq				5.2	
	3eq,4eq				5.2	
	4eq,5eq	3.2	4.0			
	5eq,6eq	3.2				
^4J W	2eq,4eq		1.9			
	2eq,6eq		1.9			

axial protons ($^3J_{ax,ax} \approx 12.0$ Hz, $^3J_{ax,eq}$ and $^3J_{eq,eq} \approx 2.5$–4.0 Hz).

The conformational analysis is based on the vicinal ^3J ^{1}H,^{1}H coupling constants reported in Table 4.

cis-C6 **1**: The spin system is complex, because the two 2-H protons are nearly isochronous (Table 2): no coupling constant is directly readable on the 250 or 500 MHz 1D spectra (Fig. 6). At 500 MHz and at pH 7.0 we could deduce the axial or

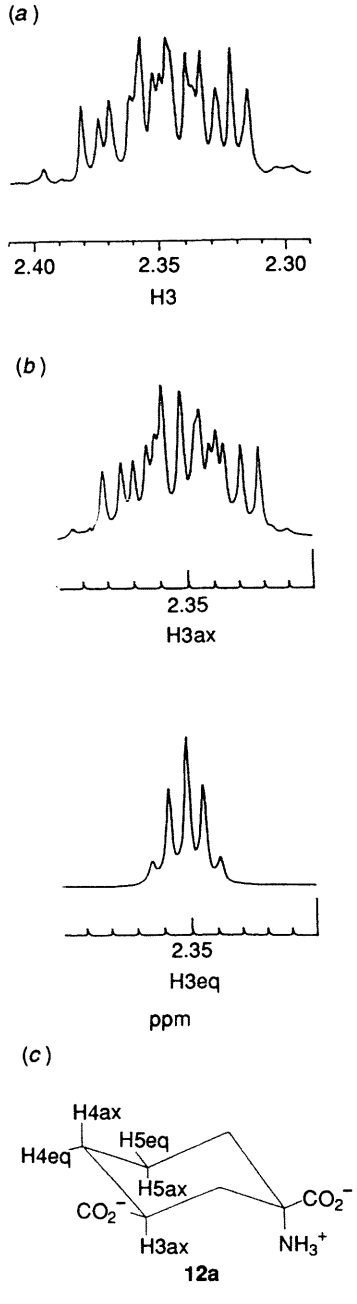

Fig. 6 (*a*) Details of the 500 MHz ^{1}H spectrum of *cis*-C6 in D_2O at pH 7.0 (**12**) (Gaussian resolution enhancement). (*b*) Simulation of the signal of 3-H in *cis*-C6 (500 MHz, linewidth 1 Hz, pH 7.0; shifts from Table 1). 3-H axial: $^2J_{ax,eq}$ −13.0, $^3J_{ax,ax}$ 11.8, $^3J_{ax,eq}$ 3.4 Hz; 3-H equatorial: $^2J_{ax,eq}$ −13.0, $^3J_{eq,ax} = {}^3J_{eq,eq}$ = 3.4 Hz. (*c*) Predominant conformation of *cis*-C6 in aqueous solution (represented at pH 7).

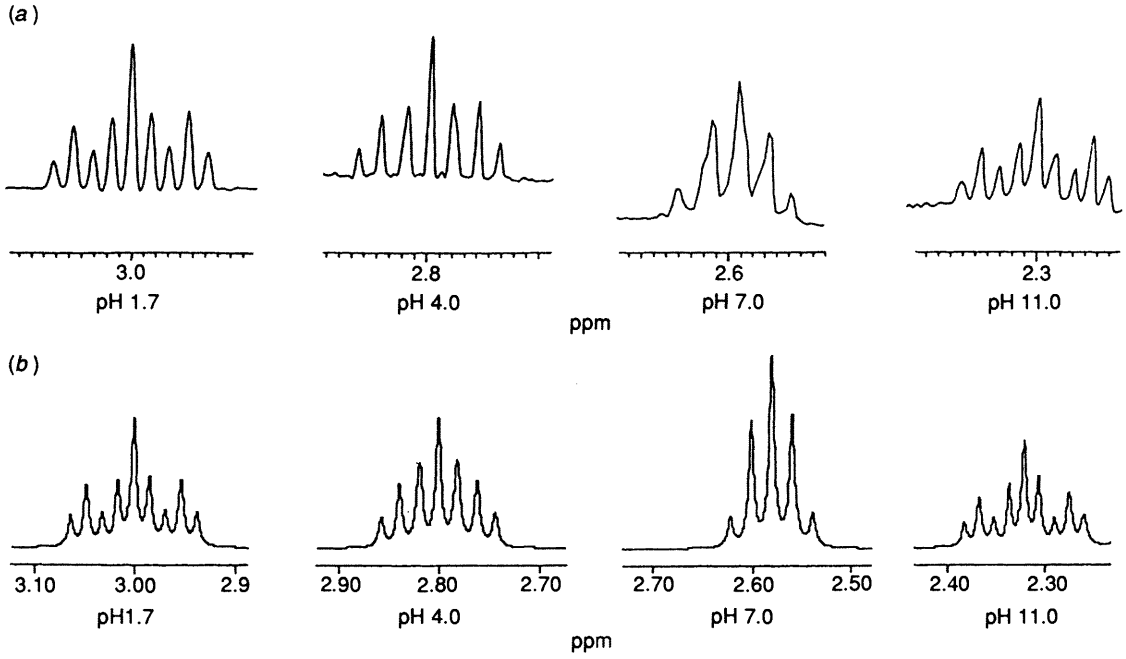

Fig. 7 (*a*) Details of the 250 MHz ^1H spectra of *trans*-C6 in D_2O at various pH values, signal of 3-H (gaussian resolution enhancement). (*b*) Simulation of the signal of 3-H in *trans*-C6 at various pH values (250 MHz, linewidth 0.8 Hz, shifts from Table 1) with the experimental coupling constants from Table 3 (with $^2J_{ax,eq}$ 13.0 Hz when not determined).

Table 5 Measured* and calculated sums of the coupling constants (Hz) of 3-H in *cis*-C6

cis-C6 **1**		
Struct.	3-H	Σ^3J
11 X-Ray	ax	32.0
11 RMN	ax	32.0*
11a MD	ax	32.0
11b MD	eq	16.0

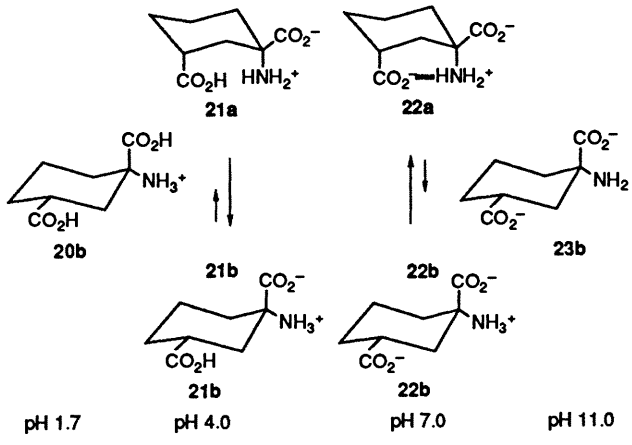

Fig. 8 Predominant conformations of *trans*-C6 in aqueous solution

equatorial position of the 3-H proton from the multiplicity of its neighbouring nucleus 4-Hax. The 4-Hax signal appears like a quartet of doublets with three large coupling constants of 12.0 (or 13.0) Hz and one smaller coupling constant of 3.4 Hz. This 4-Hax proton is thus coupled to its geminal proton 4-Heq (J −13.0 Hz) and to the vicinal protons 5-Hax and 3-Hax (J 12.0 Hz), and to the equatorial proton 5-Heq (J 3.4 Hz). Such data show that 3-H is axial; thus the two carboxylate groups are equatorial and the amino group axial: this is the **a** conformer represented in Fig. 6(*c*). This result was confirmed by spectral simulation: an equatorial proton would have resonated very differently [Fig. 6(*b*)].

At the other pHs tested, the 4-Hax signal could not be analysed owing to superpositions; but the half-height width of the 3-H signal was used as an approximation of the sum of its coupling constants.[20] At any pH it has a value of ~31 Hz, corresponding to an axial proton [$2(^3J_{ax,ax}) + 2(^3J_{ax,eq}) = 2(12.0) + 2(3.4) = 30.8$ Hz]. For an equatorial proton the width would be about 13 Hz, $2(^3J_{eq,ax}) + 2(^3J_{eq,eq}) = 2(3.4) + 2(3.2) = 13.2$ Hz.

We can conclude that the *cis*-C6 **1** always adopts the chair conformation **a** with the minimal steric hindrance represented in Fig. 6(*c*). Assuming, as a first approximation, a flattened cyclohexane chair (endocyclic torsion angle 56°) the resulting coupling constants are not very different from those for a 'perfect chair'.[21]

At isoelectric pH this corresponds to the results of X-ray crystallography (Fig. 5): in Table 5 we have reported the sums of coupling constants for 3-H observed in the *cis*-C6 isomer **11** NMR spectra and calculated by Altona's equations[22] from the X-ray structure **11a**, and from the minimized structures generated by molecular dynamics (MD) (**11a** and **11b**, see below). The experimental values for compound **11** are in good agreement with the calculated values for **11a**.

trans-C6 **2**: For this isomer the spin system is simpler because 2-H protons are anisochronous. A number of coupling constants are deduced from 1D spectra at 250 or 500 MHz, and confirmed by 2D J-resolved experiments (Table 4). The coupling constants of 3-H (the most shifted proton because of the adjacent 3-carboxy group) at various pHs is sufficient to determine the conformation of the *trans*-isomer **20** to **23**. The geminal protons 2-Hax and 2-Heq, 4-Hax and 4-Heq are anisochronous at all the pHs tested. This allows a first-order analysis of the spin sub-system formed by 2-H_2, 3-H and 4-H_2 to be made.

At pH 1.7, where all the groups are protonated, the 3-H signal looks like a triplet of triplets [Fig. 7(*a*)], in agreement with an axial proton coupled to two axial neighbours (2-Hax and 4-Hax, $^3J_{ax,ax}$ 11.9 Hz) and to two equatorial neighbours (2-Heq and 4-Heq, $^3J_{ax,eq}$ 4.0 Hz). The conformer is then **20b** (Fig. 8).

At pH 4.0 these coupling constants are averaged [9.7 and

Table 6 Longitudinal relaxation times (T_1/s) for ^{13}C in D_2O at pH 7 (error of 5%)

Carbon		*cis*-C6 **12** $T_1(NT_1)$	*trans*-C6 **22** $T_1(NT_1)$	$\Delta NT_1 \cdot 100/NT_1$ *cis*
1	C	1.1	5.5	
2	CH_2	0.5	0.8	
		(1.0)	(1.5)	+55%
3	CH	0.9	1.4	+54%
4	CH_2	0.6	0.7	
		(1.2)	(1.3)	+16%
5	CH_2	0.6	0.7	
		(1.2)	(1.5)	+26%
6	CH_2	0.4	0.6	
		(0.9)	(1.3)	+48%
7	CO	3.9	5.5	
8	CO	1.3	5.4	

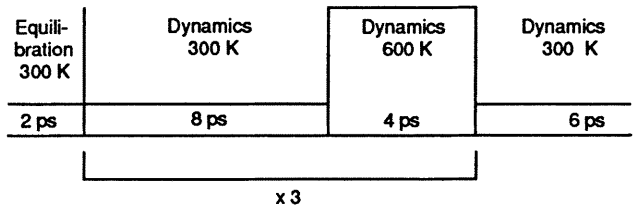

Fig. 9 Molecular dynamics protocol

4.5 Hz, Fig. 7(*a*)]: the **b** conformer is still predominant but in conformational equilibrium with the **a** conformer in which 3-H is equatorial (Fig. 8). At pH 7.0 all coupling constants become equal to 5.2 Hz [Fig. 7(*a*)], the equilibrium **a** ⇌ **b** still exists but the **a** conformer is now predominant (Fig. 8).

Using the extreme values of $^3J_{ax,ax}$ = 12.0 Hz (**b** conformation) and $^3J_{eq,eq}$ = 3.0 Hz (**a** conformation) it is possible to estimate the molar ratio x of conformer **b** at each pH:

$$J_{obs} = x(^3J_{ax,ax}) + (1 - x)(^3J_{eq,eq})$$

so

at pH 4: J_{obs} = 9.7 Hz, x = 0.75 ⇒ 75% of conformation **21b**
at pH 7: J_{obs} = 5.2 Hz, x = 0.25 ⇒ 25% of conformation **22b**.

At alkaline pH the coupling constants are similar to those measured at acidic pH (11.4 and 3.7 Hz): the 3-H proton is again purely axial and 100% of conformation **23b** is observed.

This first-order analysis of the spin-system was confirmed by spectral simulation: the sub-spectra calculated from the *J*- and *δ*-values in Tables 2 and 4 are in agreement with the experimental data [Fig. 7(*b*)]. On the other hand, at pH 4 and 7, simulations of a purely axial 3-H with coupling constants of 12.0 and 3.0 Hz, like a triplet of triplets, did not restore the experimental signal. At pH 7.0, we note that the linewidth of the experimental signal, even after Gaussian resolution enhancement [Fig. 7(*a*)], is larger than the corresponding one in the simulated spectrum [Fig. 7(*b*)]. This might be due to a small ^4JW coupling between the equatorial protons 3-Heq and 5-Heq. Therefore, at extreme pH (1.7 and 11.0), the preferred conformation is the sterically favoured one **b**, while at intermediate pH (4.0 and 7.0) a conformational equilibrium between conformers **a** and **b** occurs, the **a** conformer being very likely stabilized by an electrostatic interaction (like a hydrogen bond) between the 1-ammonium and the 3-carboxy or carboxylate groups (Fig. 8).

Comparison of ^{13}C *longitudinal relaxation times* (T_1). Information about the structural flexibility of these compounds can be experimentally obtained from the T_1 relaxation times of the carbon resonances. The NT_1-values (N = number of attached protons, T_1 = longitudinal relaxation time) correlate directly with the molecular mobility. This is due to the fact that the ^{13}C relaxation of these carbons is mainly dominated by the single relaxation mechanism, that is ^{13}C–^1H dipolar interaction with directly bonded hydrogens.[23]

The values of NT_1s measured by inversion-recovery experiments at pH 7.0 are reported in Table 6. These data provide us with information about rotational motion of the backbone of the glutamic acid derivative's molecule and about the internal rotations of the substituents. All the carbons gave very similar NT_1-values, indicating rigidity of the backbone. For each of the carbons the NT_1s are larger in the *trans*-isomer **2** than in the *cis*-isomer **1**. This shows that the atoms in *trans*-C6 **2** are more mobile than those in the *cis*-isomer **1**, perhaps confirming the occurrence of a conformational equilibrium for *trans*-C6 **2** at pH 7.0.

Molecular Dynamics.—To simulate the molecular movements in solution, different protocols have been used, following the scheme presented in Fig. 9 with the Biosym software INSIGHTII and DISCOVER. For an exploration of the conformational space, after an equilibration period of 2 ps, the dynamics are run at 300 K with periodical jumps to 600 K to supply the system with energy (to pass conformational barriers). The 42 ps trajectory is sampled every picosecond, the structures are then minimized by molecular mechanics and stored.

We have run experiments starting from each one of the possible conformations to compare their energies in case the interconversion was not observed. Considering the results of NMR experiments, particular attention had to be given to the modelling of electrostatic interactions (including hydrogen bonding), which are calculated in the force field by a coulombic expression.

First protocol. A widely used method to mimic the solvent's screening effect is to use a distance-dependent relative permittivity $\varepsilon = r$, leading to an r^2 dependence of the coulombic energy.[24] We applied it to each one of the possible conformations as starting points. The potential energies of the energy-minimized **a** or **b** conformers generated are reported in Table 7.

cis-C6 **1**: at each pH the energies of the **a** and **b** conformers were compared: at alkaline pH E(**a**) < E(**b**) (**12** and **13**), while at acidic pH the difference between conformers **10a** and **10b** is not significant. The **a** structures are stable during the whole protocol while the **12b** and **13b** forms are transformed into the **a** conformer from the beginning of the dynamics. This is coherent with the NMR results, confirming that the **a** conformer is the preponderant one in solution. However, at isoelectric pH the experiment on **11b** could not be achieved: an overestimated electrostatic attraction between the 1-carboxylate and the 3-carboxy groups led to the rupture of the molecule, with an energy minimized before equilibration smaller than that of the solution conformer **11a**.

trans-C6 **2**: the **a** and **b** conformers have energies in the same range, and no interconversion is observed (see Table 7). At alkaline pH E(**23b**) < E(**23a**), which corresponds to the results of NMR experiments (**23b** being the conformer in solution). However, the experiment aborts at pH 7.0 for **22a** (1,3-diaxial interaction between NH_3^+ and CO_2^-), and at acidic pHs the conformations **20b** and **11b**, predominant in solution according to NMR results, have energies about 5 kcal higher than those of **a** conformers.

These experiments allowed us to confirm some of the results obtained by NMR spectroscopy, but the force field seems unsuitable for characterization of the 1,3-diaxial electrostatic interactions and thus must be modified. Use of a distance-dependent relative permittivity ($\varepsilon = r$) in the absence of explicit solvent is common but it is a crude approximation to reality and it cannot deal properly with strong charge

Table 7 Minimal potential energies of the structures generated by protocol 1 (*, energy minimized before equilibration; **, experiment aborted)

cis-C6 **1**			*trans*-C6 **2**		
Starting conformation	*E***a**/kcal	*E***b**/kcal	Starting conformation	E_p**a**/kcal	E_p**b**/kcal
10b	30.0		**20a**	17.2	
10b		29.4	**20b**		22.5
11a	−0.1		**21a**	−4.2	
11b**		−4.6*	**21b**		0.3
12a	−2.2		**22a****	−18.3	
12b	−2.2	13.3*	**22b**		1.1
13a	33.7		**23a**	39.1	
13b	33.7	47.7*	**23b**		33.8

Table 8 Minimal potential energies of the structures generated by protocol 2 (*, energy minimized before equilibration)

cis-C6 **1**			*trans*-C6 **2**		
Starting conformation	E_p**a**/kcal	E_p**b**/kcal	Starting conformation	E_p**a**/kcal	E_p**b**/kcal
10a	25.7		**20a**	28.3	
10b		26.5	**20b**		23.5
11a	8.0		**21a**	9.9	
11b		11.4	**21b**		7.4
12a	6.1		**22a**	4.1	
12b	6.1	15.1*	**22b**		7.4
13a	33.2		**23a**	37.6	
13b		41.9	**23b**		33.3

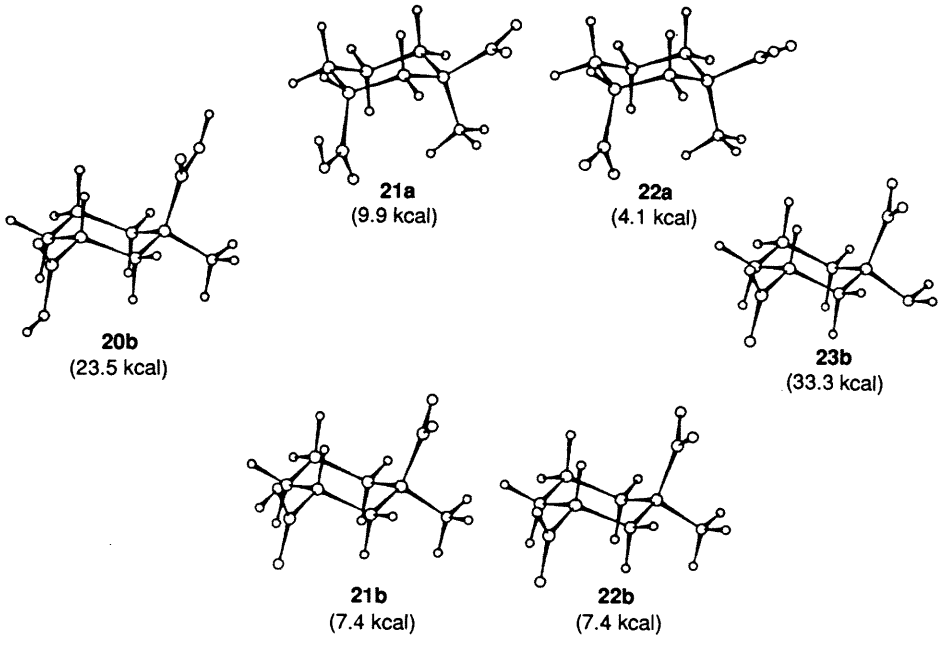

Fig. 10 Stable structures generated by the second protocol for *trans*-C6 at various pH values

interactions such as occur in these molecules. Hence the behaviour of the calculations under the first protocol is not unexpected.

Second protocol. It is possible explicitly to model the solvent effect in the vicinity of the molecules: we used the electrostatic interaction expression $E = Kq_1q_2/\varepsilon r$ and tried to adjust the relative permittivity to a value, between 1 and 78.54,[24] corresponding to the interactions in aqueous solution. We used the results of the NMR experiments on the conformational equilibrium observed for the *trans*-C6 at pH 4.0 and 7.0:

at pH 4:

21a ⇌ **21b**
25% 75%
$\Delta G°$ (300 K) −2.8 kcal

at pH 7:

22a ⇌ **22b**
75% 25%
$\Delta G°$ (300 K) +2.8 kcal

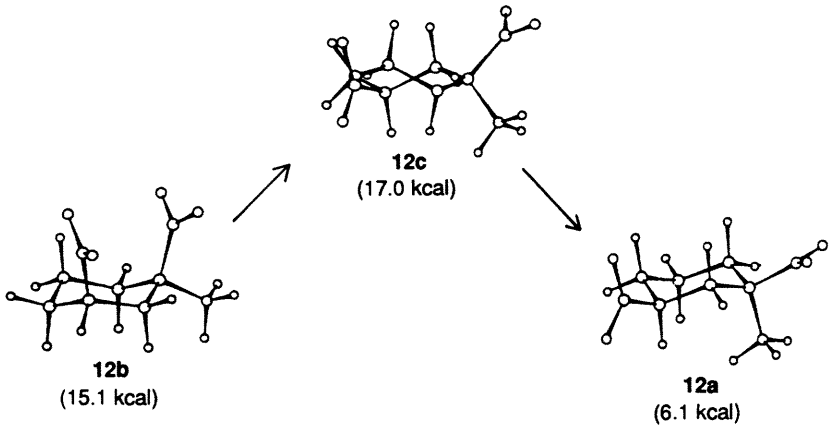

Fig. 11 Structures generated by the second protocol for *cis*-C6 at neutral pH

Table 9 Measured* and calculated coupling constants of 3-H in *trans*-C6

trans-C6 **2**									
		3-H–2-H_{trans} ($3^{ax}2^{ax}$ or $3^{eq}2^{eq}$)		3-H–2-H_{cis} ($3^{ax}2^{eq}$ or $3^{eq}2^{ax}$)		3-H–4-H_{trans} ($3^{ax}4^{ax}$ or $3^{eq}4^{eq}$)		3-H–4-H_{cis} ($3^{ax}4^{eq}$ or $3^{eq}2^{ax}$)	
Structure	3-H ax/eq	φ(°)	^3J/Hz	φ(°)	^3J/Hz	φ(°)	^3J/Hz	φ(°)	^3J/Hz
20 NMR	ax		11.8*		3.9*		11.9*		3.8*
20a	eq	71.8	1.4	−39.9	6.9	−72.0	1.4	42.2	6.4
20b	ax	176.7	13.2	62.2	2.6	−174.5	13.0	−57.8	3.4
21 NMR	ax + eq		9.7*		4.5*		9.7*		4.5*
21a	eq	70.4	1.6	−42.0	6.5	−71.9	1.4	42.5	6.3
21b	ax	176.0	13.2	61.3	2.8	−174.5	13.0	−57.8	3.4
22 NMR	ax + eq		5.2*		5.2*		5.2*		5.2*
22a	eq	69.3	1.7	−43.0	6.3	−71.7	1.4	42.7	6.3
22b	ax	173.6	13.1	59.4	3.9	−172.8	12.9	−56.5	3.6
23 NMR	ax		11.4*		3.7*		11.4*		3.7*
23a	eq	71.5	1.4	−40.8	6.7	−72.7	1.3	41.9	6.5
23b	ax	174.4	13.1	60.0	3.0	−173.6	13.0	−57.1	3.5

Table 10 Dihedral angles (°) in *cis*-C-6: comparison of the values obtained by X-ray crystallography and molecular dynamics (MD)

	11a X-Ray	**11a** MD (8.0 kcal)	**11b** MD (11.3 kcal)
Endocycle torsion angles			
C(1)–C(2)–C(3)–C(4)	−53.2	−54.3	46.4
C(2)–C(3)–C(4)–C(5)	56.8	54'8	−46.8
C(3)–C(4)–C(5)–C(6)	−58.6	−54.8	51.9
C(4)–C(5)–C(6)–C(1)	55.5	53.8	−55.5
C(5)–C(6)–C(1)–C(2)	−49.6	−51.0	53.1
C(6)–C(1)–C(2)–C(3)	49.1	49.5	−51.4
Substituents			
N(1)–C(1)–C(2)–C(3)	−71.1	−71.5	−166.6
O(2)–C(7)–C(1)–C(2)	136.8	−149.1	44.9
O(1)–C(7)–C(1)–C(2)	−45.9	33.5	−135.8
C(7)–C(1)–C(2)–C(3)	170.7	173.8	79.0
C(7)–C(1)–C(2)–H(2)$_{(1)}$	45.2	52.1	−48.0
C(7)–C(1)–C(2)–H(2)$_{(2)}$	−65.7	−62.4	−162.0
O(3)–C(8)–C(3)–C(4)	−121.7	−56.5	124.9
O(4)–C(8)–C(3)–C(4)	59.4	123.8	−54.3
C(8)–C(3)–C(4)–H(4)$_{(1)}$	51.5	56.2	−39.4
C(8)–C(3)–C(4)–H(4)$_{(2)}$	−55.5	−60.4	−153.5

We have run dynamics starting from each of these four conformers (**21a**, **21b**, **22a**, **22b**), with different values of ε. Correct energy differences between the **a** and **b** forms are obtained for $\varepsilon = 5$. With this value of the relative permittivity, experiments are run starting from each one of the possible chairs for the two isomers. The results are summarized in Table 8.

trans-C6 **2**: the results are in good agreement with NMR results at intermediate pHs:

$$\mathbf{21a} \rightleftharpoons \mathbf{21b} \quad \text{with } E_p\mathbf{b} - E_p\mathbf{a} \approx -2.5 \text{ kcal}$$

$$\text{and } \mathbf{22a} \rightleftharpoons \mathbf{22b} \quad \text{with } E_p\mathbf{b} - E_p\mathbf{a} \approx +3.3 \text{ kcal}$$

At extreme pHs, the electrostatic interactions are not important and the **b** conformers have the lower energies, which corresponds to the NMR results (Fig. 10). The energies are thus in the same range as in the first protocol, because the sterical parameters have not been modified.

No interconversion has been observed.

The coupling constants for 3-H (γ-CH) were calculated from the dihedral angles for each conformer generated by molecular dynamics. They are in good agreement with those obtained from NMR spectra (Table 9).

cis-C6 **1**: at each pH considered, the **a** and **b** conformers are stable, and the energy of the **a** conformer is lower, confirming the results of NMR experiments. Only in one case was an interconversion observed, at neutral pH where the **12b** conformer leads immediately to the more stable conformer **12a** *via* a twist-boat intermediate **12c** (Fig. 11).

The most significative dihedral angles of the minima for **11a** and **11b** were measured and compared with the values of the crystalline structure (Tables 5 and 10): obviously, the values for **11a** are very close to the X-ray data, while the conformation **11b** is totally different.

The stability of the different conformers of *cis*- and *trans*-C6 has been tested at pH 7 by a 100 ps dynamics protocol at 300 K. All the dihedral angles measured varied less than 1° during the dynamics, except that the oxygen atoms exchange their positions in the α- and γ-carboxylate groups by 180° rotation.

The second protocol, in which one experimental result is used to select a value of the relative permittivity to make calculations agree with experiment, is a preferred choice. It is understood that such a choice has little or no physical meaning and will be applicable only over a limited range of structures. For the other molecules, a protocol with explicit modelling of water is the preferred choice and, in this case, the appropriate value of the relative permittivity is 1. However, it is not of practical use: the CPU times are much longer than for a single molecule, and the energies obtained are those of C6 + H_2O systems; thus the energies of the minimized C6 molecules themselves are very difficult to evaluate. Therefore, we conceived a protocol avoiding the introduction of explicit water molecules, which would rapidly give results in conformational studies in other series of glutamic acid derivatives.

Conclusions.—The results of X-ray crystallography, ^1H and ^{13}C NMR spectroscopy, and molecular dynamics are in good agreement: the amino group in the *cis*-C6 is found to be axial at every pH (**a** conformer): both carboxy groups are equatorial to reduce the sterical energy.

In the *trans*-C6 the steric parameters favour the **b** conformers in which the amino group is equatorial at acidic and alkaline pHs, while at intermediate pH (in particular around pH 7) a 1,3-electrostatic attraction stabilizes the **a** conformer.

Both isomers are thus shown to adopt well defined conformations and prove to be well adapted for comparative structure–activity correlation studies.

Some NMR data have been necessary to optimize a molecular dynamics protocol that can now be used directly and rapidly for the conformational analysis in water of other charged molecules of a similarly limited size, for which a protocol, adapted to proteins or other large molecules, is not really convenient.

Experimental

Materials.—*cis*-**1** and *trans*-**2**-C6 have been previously prepared in the laboratory.[25] Only racemates have been used for this work.

X-Ray Crystallography.—*Crystal data for* cis-*C6* **1** *hemihydrate.* $C_8H_{13}NO_4 \cdot 1/2H_2O$, M = 187.2. Monoclinic, a = 10.255(2), b = 6.479(1), c = 28.171(3) Å, β = 96.0(2)°, V = 1861.5(9) Å^3, space group $C2/c$, Z = 8, D_c = 1.41 g cm^{-3}, final R-value 0.050, final R_w-value 0.054.

X-Ray structure determination of cis-*C6* **1** *hemihydrate.* Crystals of compound **1** hemihydrate were grown by slow evaporation of an acetone–water solution. Philips PW 1100 diffractometer, θ–2θ scan mode up to θ = 28°, graphite-monochromated Mo-Kα radiation (λ = 0.710 69 Å); 2178 unique reflections; 1186 reflections with $F \geqslant 7\sigma(F)$ considered observed. The structure was solved by SHELXS86[26] and refined by full-matrix blocked least-squares with weight $w = 1/[\sigma^2(F) + 0.001\,14\,F^2]$. The thermal parameters were anisotropic for all non-hydrogen atoms. The hydrogen atoms were all found on a difference-Fourier map (except that of the water molecule) and isotropically refined. All calculations were performed on the Micro VAX3400 Digital computer of the University of Padova using SHELX-76.[27]*

NMR Spectroscopy.—The samples were dissolved in deuterium oxide at a saturation concentration of 0.01 mol dm^{-3}; the pH (in fact pD = pH − 0.4, uncorrected here) was adjusted by addition of DCl or NaOD. At pH 7 the samples have been dissolved in an aq. NaD_2PO_4/Na_2DPO_4 buffer (0.5 mol dm^{-3}), and concentrations of 0.04 mol dm^{-3} for the ^1H experiments and 0.15 mol dm^{-3} for the ^{13}C experiments could be attained. Degassed and sealed tubes were used for the T_1 determinations.

The errors in the chemical shifts are 0.01 and 0.1 ppm for ^1H and ^{13}C, respectively. A crystal of 3-(trimethylsily)[2,2,3,3-$^2H_4$]propionic acid, sodium salt ([$^2H_4$]TSP) was used as internal reference for the proton shifts, and for the carbon a value of the absolute frequency was used. The coupling constants are given with a precision of 0.5 Hz.

The experiments were run at 250 and 500 MHz for ^1H, and 62.9 MHz for ^{13}C, on Bruker WM 250 and AM 500 spectrometers, at room temperature. The data processing was done on a PC computer using the Bruker software WIN-NMR, and the spectrum simulation on a Macintosh II computer using the software NMR″II.

Presaturation of the solvent with two decoupling powers was used for all the 1D and 2D ^1H experiments.

The DEPT polarization transfer from ^1H to ^{13}C nuclei with decoupled spectra was acquired and turned for optimum polarization transfer with $^1J_{CH}$ 135 Hz. The 2D ^1H,^1H COSY spectra were acquired with a spectral width of 1500 Hz into 512 data points in f_2, and with 64 experiments (f_1). The 90° pulse was 5.7 μs, the relaxation delay 1 s, and each FID was acquired with 64 scans and 2 dummy scans. The data were zero-filled to 1024 and 512 points in f_2 and f_1, respectively, prior to double Fourier transformation with an unshifted sine-bell window function in both dimentions.

The 2D ^1H, ^{13}C COSY experiments data were acquired with sweep widths and data points of 2500 Hz and 1024 points, and 600 Hz and 64 data points (for ^1H and ^{13}C, respectively). The 90° pulses were 7.7 μs for ^1H and 12.0 μs for ^{13}C. Each FID was acquired with 512 scans and a relaxation delay of 1.2 s. This experiment gave ^1H decoupling in f_2 and C–H shift correlation with ^1H decoupling in the f_1 domain except for geminal ^2J. This experiment was tuned for optimum polarization transfer with again the value of $^1J_{CH}$ 135 Hz.

The homonuclear J-resolved 2D NMR data, using the Hahn spin-echo, were acquired with sweep widths and data points of 1400 Hz and 8K points in the f_2 domain (for chemical shifts, after tilt), and 44 Hz and 32 points in the f_1 domain (for homonuclear couplings).

The ^{13}C T_1 relaxation-time measurements used an inversion-recovery pulse sequence with a relaxation delay of 7 s and averaging 512 scans into a 16K data block. The experiment was repeated for 10 values of the variable-delay (VD) ranging from 0.01 to 10 s. The T_1-values were calculated by using the Bruker DISNMR program. The calibrated value of the 180° pulse was 24.0 μs.

Molecular Dynamics.—The calculations were run on a Silicon Graphics 4D/20 computer using the Biosym software INSIGHTII and DISCOVER. The stuctures were derived from the crystallographic co-ordinates of the solid *cis*-C6 as a starting point and the substituents and the charges were modified. The structures were minimized ('steepest descent' and 'conjugate gradients' steps, until convergence), then equilibrated at 300 K for 2 ps (variable-temperature protocols) or 4 ps (constant-temperature protocols). The dynamics were run for 42 ps (variable temperature) or 100 ps (constant temperature); the trajectory was sampled by minimizing and storing of the

* *Supplementary data* (see Instructions for Authors (1993), section 5.6.3, issue 1). Tables of fractional atomic coordinates, bond lengths, and bond angles are available from the Cambridge Crystallographic Data Centre.

structure every picosecond. Coupling constants were calculated from the torsion angles using the software ALTONA on a Macintosh II computer.

Acknowledgements

We thank Francois Trigalo for the preparation of the cyclohexane-derived analogues of glutamic acid, and CNRS for financial support.

References

1 K. Shimamoto, M. Ishida, H. Shinozaki and Y. Ohfune, *J. Org. Chem.*, 1991, **56**, 4167.
2 J. D. Gass and A. Meister, *Biochemistry*, 1970, **9**, 842.
3 V. A. James, R. J. Walker and H. V. Wheal, *Br. J. Pharmacol.*, 1980, **68**, 711; J. G. Hall, T. P. Hicks, H. McLennan, T. L. Richardson and H. V. Wheal, *J. Physiol.*, 1979, **286**, 29; H. V. Wheal and G. A. Kerjut, *Comp. Biochem. Physiol.*, 1976, **53C**, 51; G. A. R. Johnston, D. R. Curtis, J. Davies and R. M. McCulloch, *Nature (London)*, 1974. **248**, 804.
4 F. Acher, N. Morelle, J. Gharbi-Benarous, J. P. Girault and R. Azerad, unpublished data.
5 F. Archer, N. Morelle, J. Gharbi-Benarous, G. Valle, M. Crisma, C. Toniolo, R. Azerad and J. P. Girault, *Peptides*, eds. C. H. Schneider and A. N. Eberle, ESCOM, 1993.
6 C. K. Johnson, ORTEP II, Report ORNL-5138, Oak Ridge National Laboratory, Tennessee, USA, 1976.
7 G. Valle, M. Crisma, C. Toniolo, N. Sen, M. Sukumar and P. Balaram, *J. Chem. Soc., Perkin Trans. 2*, 1988, 393.
8 K. K. Chacko, R. Srinivasan and R. Zand, *J. Cryst. Mol. Struct.*, 1971, **1**, 261.
9 M. Bixon and S. Lifson, *Tetrahedron*, 1967, **23**, 769.
10 D. Cremer and J. A. Pople, *J. Am. Chem. Soc.*, 1975, **97**, 1354.
11 IUPAC–IUB Commission on Biochemical Nomenclature, *Biochemistry*, 1970, **9**, 3471.
12 J. Mitra and C. Ramakrishnan, *Int. J. Pept. Protein Res.*, 1977, **9**, 27.
13 I. D. Brown, *Acta Crystallogr., Sect. A*, 1976, **32**, 24.
14 C. Ramakrishnan and N. Prasad, *Int. J. Protein Res.*, 1971, **3**, 209.
15 R. Taylor, O. Kennard and W. Versichel, *Acta Crystallogr., Sect. B*, 1984, **40**, 280.
16 C. H. Görbitz, *Acta Crystallogr., Sect. B*, 1989, **45**, 390.
17 M. R. Bendall and D. T. Pegg, *J. Magn. Reson.*, 1983, **53**, 272.
18 A. Bax and R. Freeman, *J. Magn. Reson.*, 1981, **44**, 542.
19 J. A. Rutar, *J. Magn. Reson.*, 1984, **59**, 306; T. C. Wong and V. Rutar, *J. Am. Chem. Soc.*, 1984, **106**, 7380.
20 L. M. Jackman and S. Sternhell, *Applications of Nuclear Magnetic Resonance Spectroscopy in Organic Chemistry*, Pergamon Press, Oxford, 2nd edn., 1969, p. 114.
21 C. A. G. Hasnoot, F. A. A. M. De Leeuw and C. Altona, *Tetrahedron*, 1980, **36**, 2783.
22 C. Altona and M. Sudaralingam, *J. Am. Chem. Soc.*, 1973, **95**, 2333.
23 A. Allerhand, D. Dodrell and R. Komoroski, *J. Chem. Phys.*, 1971, **55**, 189; J. R. Lyerla and G. C. Levy, *Top. Carbon-13 NMR Spectrosc.*, 1974, **1**, 79.
24 S. K. Burt, D. Mackay and A. T. Nagler, in *Computer-Aided Drug Design*, ed. T. J. Perun and C. L. Propst, Marcel Dekker, New York and Basel, 1989, p. 66.
25 F. Trigalo, D. Buisson and R. Azerad, *Tetrahedron Lett.*, 1988, **29**, 6109.
26 G. M. Sheldrick, SHELXS 86. Program for Crystal Structure Determination, University of Göttingen, 1986.
27 G. M. Sheldrick, SHELX-76. *Program for Crystal Structure Determination*, University of Cambridge, 1976.

Paper 2/05154K
Received 25*th September* 1992
Accepted 11*th November* 1992